2020 年度学位申請論文

Short-term high-fat diet intake leads to exacerbation of concanavalin A-induced liver injury through the induction of procoagulation state.

短期間の高脂肪食摂取は凝固亢進状態の誘導により
コンカナバリン A 誘発性肝障害の増悪をもたらす

名古屋大学大学院医学系研究科
医療技術学専攻
病態解析学分野

（指導：石川　哲也　教授）
名仁澤　英里

Short-term high-fat diet intake leads to exacerbation of concanavalin A-induced liver injury through the induction of procoagulation state.

短期間の高脂肪食摂取は凝固亢進状態の誘導によりコンカナバリン A 誘発性肝障害の増悪をもたらす

Eri Nanizawa

Program in Radiological and Medical Laboratory Sciences, Pathophysiological Laboratory Sciences

Academic adviser: Tetsuya Ishikawa

Abstract

Obesity and high-fat diet (HFD) are known to cause proinflammatory and procoagulation states and suggested to become a risk of developing thromboembolic diseases. Non-alcoholic fatty liver disease (NAFLD) is usually associated with obesity and HFD, and a part of NAFLD is known to progress to nonalcoholic steatohepatitis (NASH), the pathogenesis of which has not been fully elucidated. In the current study, we examined the influence of short-term HFD on hepatic expression of the molecules related to inflammation, coagulation, metabolism, and cellular stresses from the perspective that HFD itself can be a risk for the development to NASH. In the analysis in short-term (4 days to 14 days) HFD-fed mice, we found out that HFD increased hepatic expression of IFN-γ, TNF-α, IL-10, monocyte chemotactic protein-1 (MCP-1), tissue factor (TF), plasminogen activator inhibitor-1 (PAI-1) mRNAs, and fibrin/fibrinogen deposition in the liver tissues. And it was suggested that metabolic alterations and endoplasmic reticulum (ER) stresses induced by the HFD intake were associated with this proinflammatory and procoagulation states. When we administered concanavalin A (Con A) to these HFD-fed mice, the extent of liver injury was dramatically exacerbated in HFD-fed mice. Heparin treatment to Con A-administered, HFD-fed mice (for 4 days) profoundly ameliorated the extent of liver injury. These suggest that even short-term of HFD intake induces proinflammatory and procoagulation states in the liver and thereby increases the susceptibility of the liver to circulating inflammatory stimuli. We think that it may explain a part of NASH pathogenesis.

短期間の高脂肪食摂取は凝固亢進状態の誘導によりコンカナバリン A 誘発性肝障害の増悪をもたらす

医学系研究科　医療技術学専攻　病態解析学分野　名仁澤　英里
指導教員　石川 哲也

肥満および高脂肪食（HFD）摂取は、炎症および凝固亢進状態を引き起こすことが知られており、血栓性疾患を発症するリスクになることが示唆されている。一般的に、非アルコール性脂肪肝疾患（NAFLD）は、肥満と HFD 摂取に関連しており、NAFLD の一部は非アルコール性脂肪肝炎（NASH）に進行することが知られているが、その病因は完全には解明されていない。本研究では、HFD 摂取自体が NASH の発症のリスクになる可能性があるという観点から、短期 HFD 摂取における、炎症、凝固、代謝、細胞ストレスに関連する分子の肝内遺伝子発現に及ぼす影響を調査した。短期（4 日から 14 日）HFD 給餌マウスの分析では、短期の HFD 摂取が肝内の IFN-γ、TNF-α、IL-10、MCP-1 の遺伝子発現を増加させることを発見した。また、組織因子（TF）、プラスミノゲンアクチベータインヒビター1（PAI-1）の遺伝子発現や、肝組織におけるフィブリン/フィブリノーゲン沈着の亢進が認められた。さらに、HFD 摂取により誘導される代謝変化と小胞体（ER）ストレスが、炎症および凝固亢進状態に関連していることが示唆された。また、コンカナバリン A（Con A）をこれらの短期 HFD 摂取マウスに投与すると、通常食を摂取していたマウスに比べ、肝障害の程度は劇的に悪化した。 しかし、Con A を投与した短期（4 日間）HFD 給餌マウスに、抗凝固剤であるヘパリンを投与すると、肝障害の程度を大幅に改善した。これらは、短期間の HFD 摂取でさえ肝臓の炎症および凝固亢進状態を誘発し、それにより炎症刺激に対する肝臓の感受性を増加させることを示唆しており、これは NASH の病態成立の一部を説明するものであると考える。

Contents

Introduction

In obesity, adipose tissues release TNF-α, IL-6, MCP-1, and PAI-1, causing proinflammatory and procoagulation states [1]. In addition, it has been reported that plasma levels of coagulation factors (F) VII, VIII, XII, fibrinogen, and PAI-1 are increased in obese subjects [2,3].
Epidemiological studies have shown a positive relationship between HFD intake and obesity [4]. And it has recently been reported in mice model that relatively short-term (for 14 days) HFD intake also induces increase of plasma levels of inflammatory cytokines (IL-1α, IL-6, and IL-12) and coagulation factors (fibrinogen, coagulation factor II (FII), coagulation factor VII (FVII), etc.) [5]. This suggests that HFD intake itself causes proinflammatory and procoagulation states and leads to the complication seen in the obesity, such as thromboembolic cardiovascular events.

Since obesity is frequently accompanied by NAFLD, it is not surprising that procoagulation state is present in patients with NAFLD, and that it affects the course of the disease.

NAFLD is classified into nonalcoholic fatty liver (NAFL) and nonalcoholic steatohepatitis (NASH); the latter sometimes leads to liver cirrhosis and liver cancer [6].

When the disease concept of NASH was established, "two hit theory" was proposed to explain the pathogenesis mechanism of the disease. Namely, "the first hit," hepatic steatosis, increases susceptibility of hepatocytes to the damage mediated by "the second hits," such as inflammatory cytokines/adipokines (TNF-α, MCP-1, PAI-1, etc.), adipokine imbalance, oxidative stress/mitochondrial dysfunction, ER stress, gut-derived endotoxin, and secondary bile acid. And these "two hits" are thought to contribute to the development of steatohepatitis and subsequent liver fibrosis cooperatively [7]. Recently, "multiple parallel hit theory" in which multiple parallel factors including so-called "first hit" and "second hits" act simultaneously and synergistically to induce NAFLD/NASH, is more widely accepted [8]. But the mechanism of the pathogenesis of NASH has not been fully clarified.

Con A is a lectin known to induce acute liver injury in rodents through the modulation of migrating inflammatory cells and hepatic non-parenchymal cells, including T cells, monocytes, Kupffer cells (KCs), liver sinusoidal endothelial cells (LSECs), and hepatic stellate cells (HSCs) [9-14]. When administered in mice, Con A binds to receptors of KCs and LSECs, and these Con A-bound cells stimulate T cells to secrete immunogenic cytokines such as IFN-γ and TNF-α, which subsequently induce apoptotic cell death in hepatocytes [12]. Moreover, it has been demonstrated that binding of Con A stimulates HSCs to produce IFN-γ, TNF-α, melanoma growth stimulating activity, alpha (GRO1), and interferon gamma-induced protein 10 (IP-10), resulting in the recruitment and activation of inflammatory cells, including T cells, natural killer T (NKT) cells, and neutrophils, all of which contribute to the development of acute liver injury [13,14]. In addition, it has been reported that IFN-γ and TNF-α produced from Con A-stimulated cells increase hepatic expression of TF and PAI-1, resulting in the induction of procoagulation state which causes thrombus formation in sinusoids and extensive liver necrosis [15].

It has also been demonstrated that recruitment and activation of liver-resident and non-resident cells, including T cells, neutrophils, NK cells, KCs, LSECs, and HSCs, are involved in the developing process from NAFL to NASH [16,17]. Since most of these cell lineages were involved

in the pathogenesis process of Con A-induced liver injury, we thought that it appropriately reproduces the events induced by so-called “second hits” in the NASH pathogenesis.

In the current study, we examined if short-term HFD intake caused proinflammatory and procoagulation states in the liver, and if it caused exacerbation of liver damage in the mouse model of Con A-induced liver injury

Materials and Methods

1. Animals and diet compositions

C57BL/6 male mice of 5 to 6 weeks of age were obtained from Japan SLC Inc. (Shizuoka, Japan), and housed in a controlled environment (12 hours light/dark cycles at 25ºC). They were fed with normal diet (ND: CE2, CLEA Japan Inc., Tokyo, Japan) as baseline diet, and subsequently fed with HFD (High Fat Diet 32, CLEA Japan Inc.) for certain period depending on the experimental designs. The compositions of the diets are summarized in Table 1. All the experiments were done using mice of 8 weeks of age, and five groups of mice were prepared for the experiments: ND, mice fed with ND only; HFD1, mice fed with HFD for 1 day; HFD2, mice fed with HFD for 2 days; HFD4, mice fed with HFD for 4 days; HFD14, mice fed with HFD for 14 days before becoming 8 weeks of age. Bleeding from the orbital veins and sacrifice of mice were done under anesthesia with isoflurane (Pfizer Japan Inc., Tokyo, Japan). All conditions and handing of animals in this study were conducted under the protocols approved by Nagoya University (approval number 031-036).

2. Influence of diet consumption

Three groups of mice: ND, HFD4, and HFD14 (n=5, respectively) were bled and sacrificed at 8 weeks of age (Fig. 1A). The sera and resected livers of the mice were subjected to the analyses: sera for biochemical and coagulation-related tests, and resected livers for analyses of histology and mRNA expression levels of the genes related to cytokine/chemokine, cell surface marker, coagulation, metabolism, and cellular stresses. To examine the plasma levels of coagulation-related factors, four groups of mice: ND, HFD1, HFD2, and HFD4 (n=4, respectively) were bled at 8 weeks of age, and collected plasma was subjected to the analysis (Fig. 1A). Collection of blood and liver sections was performed under fed condition to avoid changes in biochemical data and hepatic gene expression caused by fasting.

3. Concanavalin A-induced liver injury in ND- and HFD-fed mice

Three groups of mice: ND, HFD4, and HFD14 (ND, n=5; HFD4, n=6; HFD14, n=6) under fed condition, were intravenously administered with 10 mg/kg body weight of Con A (Fujifilm Wako Pure Chemical Corp. (Fujifilm Wako), Osaka, Japan) dissolved in phosphate-buffered saline (PBS, Fujifilm Wako). The final administration dose of Con A solution was of 200 µl/25 g body weight. Five mice from each group (ND, HFD4, and HFD14) were administered with PBS only (200 µl), and served as controls. Twenty-four hours after Con A or PBS administration, all the mice were bled and sacrificed. The sera and resected livers of all the mice were subjected to the analyses (Fig. 3A).

For the time-course experiment, ND and HFD4 mice administered with Con A (n=21 for each group) were bled and sacrificed at 1, 3, 24 hours after Con A administration (n=6 for controls without Con A administration, and n=5 for the individual time points, in both ND and HFD4, Fig. 4A). The sera and resected livers of all the mice were subjected to the analyses.

4. Treatment with heparin against Concanavalin A-induced liver injury

ND and HFD4 mice (ND, n=6; HFD4, n=7) were subcutaneously injected with 5,000 U/kg body weight of heparin (Novo-Heparin, Mochida Pharmaceutical, Tokyo, Japan) 30 minutes before Con A (10mg/kg body weight) administration. ND and HFD4 mice (n=6, respectively) injected with the same volume of PBS instead of Con A were served as controls. All the mice were bled and sacrificed at 24 hours after Con A administration (Fig. 5A). Serum samples and resected livers of all the mice were subjected to the analyses.

5. Biochemical and coagulation-related tests

Sera were subjected to biochemical tests: alanine aminotransferase (ALT), total cholesterol (T-Cho), triglyceride (TG), and glucose (Glu) levels, and plasma to coagulation-related tests: fibrinogen and D-dimer levels. Measurement of these items was entrusted to SRL Inc. (Tokyo, Japan).

6. Histological analysis

Liver tissues of sacrificed mice were fixed in 10 N formaldehyde (Mildform, Fujifilm Wako), embedded in paraffin, and sectioned at 3 μm thickness. The tissue sections were stained with haematoxylin & eosin (H&E), or used for immunostaining of fibrinogen/fibrin or 8-hydroxy-2'-deoxyguanosine (8-OHdG), according to the protocol provided by the manufacturer (Cell Signal Technology (CST), Inc., MA, USA). For the immunostaining, rabbit anti-fibrinogen antibody (#189490, Abcam plc, Cambridge, UK) or Anti-8-OHdG polyclonal antibody (bs-1278R, Bioss Antibodies Inc., MA, U.S.A.) was used as a primary antibody, and SignalStain® Boost IHC Detection Reagent (HRP, Rabbit, #8114, CST, Inc.) as a secondary antibody. It should be noted that the primary antibody for fibrinogen/fibrin immunostaining (#189490) does not distinguish between fibrinogen and fibrin. In order to stain liver fat, unfixed liver tissue was embedded with O.C.T. Compound (Sakura Finetek Japan, Tokyo, Japan) and frozen in liquid nitrogen to prepare a frozen specimen. Oil Red O staining was used for fat staining.

7. Quantitative reverse transcription polymerase chain reaction (qRT-PCR)

Quantitative real-time reverse-transcription polymerase chain reaction (qRT-PCR) was performed using total RNA prepared from resected mouse livers with NucleoSpin RNA (Macherey-Nagel GmbH & Co. KG, Düren, Germany). The RNA was subjected to first-strand cDNA synthesis using PrimeScript RT Master Mix (Takara Bio Inc., Shiga, Japan) according to the manufacturer's instructions. qRT-PCR was performed with Thermal Cycler Dice® Real Time System II (Takara Bio Inc.) using TB Green Premix Ex Taq II (Tli RNaseH Plus, Takara Bio Inc., Shiga, Japan) and ROX Reference Dye (Takara Bio Inc.). The PCR amplification was conducted as follows; an initial denaturing step, at 95 ºC for 30 seconds; followed by 40 cycles, at 95 ºC for 5 seconds; at 60 ºC for 31 seconds. Each sample was analyzed in duplicate. Measured genes (glycolysis-related enzymes, cytokines/chemokines, cell surface markers, coagulation-related molecules, ER stress-related molecules, hypoxia and oxidative stress-related molecules) and their primers are listed in

Table 2.

8. Statistical analysis

All the values were expressed as the mean ± SD (standard deviations). Data were analyzed by Mann-Whitney U tests for two group comparison or two-way analysis of variance test (ANOVA) followed by Steel-Dwass tests for multiple group comparison. All statistical analyses were performed with EZR (Saitama Medical Center, Jichi Medical University, Saitama, Japan), which is a graphical user interface for R (The R Foundation for Statistical Computing, Vienna, Austria). P values less than 0.05 were considered statistically significant.

Results

1. Alteration of biochemical and coagulation-related tests, and liver histology by HFD feeding

We analyzed the influence of short-term HFD intake on biochemical and coagulation- related tests, and liver histology. In the serum biochemical tests, ALT levels were not different between ND, HFD4, and HFD14 mice, while the levels of T-Cho, TG, and Glu mostly increased in HFD-fed mice compared with those in ND mice (n=5, respectively). No significant difference was found in any of the items between HFD4 and HFD14 mice (Fig. 1B, Suppl Table 1). In correspondence to these results, body wait significantly increased in HFD4 and HFD14 compared with that in ND ($p<0.05$ Suppl Table 1).

In the plasma coagulation-related tests, D-dimer levels remained under detection level in all the samples (ND, HFD1, HFD2, and HFD4) suggesting that fibrin degeneration as well as fibrin clot formation did not occur during HFD intake for 4 days. Fibrinogen levels tended to be low in HFD1 and HFD2 mice compared with those in ND mice, and fibrinogen levels in HFD4 mice showed tendency to recover to the levels in ND mice (Table 2).

In the H&E stained liver histology, fat depositions in hepatocytes and inflammatory changes in the liver, such as degeneration of hepatocytes and inflammatory cell infiltration, did not seem obvious in all the group of mice (Fig. 1C). However, Oil Red O staining showed deposition of small fat droplets in most of the hepatocytes in HFD4 and HFD14 mice. The extent of fat deposition did not seem different between the two groups of mice (Fig. 1D). The immunostaining for fibrinogen/fibrin showed extensive deposition of fibrinogen/fibrin in the liver sinusoids, especially in line with their walls, in HFD4 and HFD14 mice, while it was not evident in ND mice (Fig. 1C). It was thought that appearance of the fibrinogen/fibrin deposition in the sinusoids related to the temporal decrease in the plasma fibrinogen levels in HFD-fed mice, meaning the possibility that the deposition observed in the sinusoids were derived from plasma fibrinogen.

2. Alteration of hepatic mRNA expression patterns related to metabolism

In the mRNA expression analysis of glycolysis-related enzymes, hexokinase-4 (HK- 4) and glucose-6-phosphatase isomerase (GPI-1) mRNA levels showed significant increase in HFD-fed mice compared with those in ND mice (HK-4: ND vs. HFD4, $p<0.05$; GPI-1: ND vs. HFD4 and HFD14, $p<0.05$, respectively), suggesting the acceleration of glycolysis pathway in HFD-fed mice. Significant decrease of pyruvate dehydrogenase kinase 4 (PDK4) mRNA levels were observed in HFD-fed mice compared with those in ND mice ($p<0.05$), and it also suggests the acceleration of glycolysis pathway in HFD-fed mice. On the other hand, the decrease of PDK4 mRNA expression suggests suppression of fatty acid β-oxidation, and increase of free fatty acid and triglyceride synthesis, suggesting the association with the biochemical and histological findings in HFD-fed mice [18,19] (Fig. 2).

Although increase of serum Glu, T-Cho, and TG levels suggests the presence of insulin resistance, efficiency of Glu metabolism were not seriously disturbed considering mRNA expression patterns of the glycolysis-related enzymes. Since the development of insulin resistance is a key factor that leads to NAFLD and NASH, performing insulin resistant test need to be

considered in further study.

3. Alteration of hepatic mRNA expression patterns related to cytokine/chemokine, cell surface marker, and coagulation

We analyzed the hepatic mRNA expression of inflammatory cytokines/chemokines, cell surface markers of bone marrow-derived inflammatory cells, and coagulation-related factors in ND- and HFD-fed mice. The mRNA expression of inflammatory cytokines/chemokines such as IFN-γ, TNF-α, MCP-1, and IL-10 showed significant increase in the HFD-fed mice (HFD4 and/or HFD14) compared with ND mice ($p<0.05$). However, mRNA levels of IL-1 and IL-6 were not different between three groups of mice.

In the analysis of mRNA levels of cell surface markers, CD11b and F4/80 mRNA levels were significantly elevated in HFD14 mice compared with those in ND mice ($p<0.05$). And Ly6G mRNA levels markedly increased in HFD14 mice compared with those in ND and HFD4 mice ($p<0.05$). The results suggest the increase of monocyte, NK cell, and neutrophil migration and KC expansion in the livers of HFD14 mice. Since these does not necessarily correspond to the histology, we should consider immunostaining of liver tissues or flow cytometric analysis for liver-infiltrating or resident inflammatory cells to confirm the results in the further study. Anyway, mRNA expression patterns of both cytokines/chemokines and cell surface markers suggest the induction of inflammatory responses in the liver by the short-term HFD diet (Fig. 2).

We examined mRNA levels of TF, PAI-1, and fibrinogen-α (Fbg-α) as coagulation- related factors, which are known to be augmented by inflammatory response [20]. TF and PAI-1 mRNA levels significantly increased in HFD14 mice ($p<0.05$), and TF mRNA levels tended to increase in HFD4 mice, compared with those of ND mice ($p=0.064$). In contrast, Fbg-α mRNA levels significantly decreased in HFD4 and HFD14 mice compared with that in ND mice. The decrease of fibrinogen mRNA levels in HFD-fed mice is possibly explained by downregulation due to the elevated extracellular sterols (cholesterol and 25-hydroxycholesterol) [21] (Fig. 2).

4. Alteration of hepatic mRNA expression patterns related to cellular stresses

ER stress pathway is known to be influenced by the alteration of metabolism, trigger inflammatory reactions, and associate with the development of NASH [22]. Therefore, in order to examine the involvement of ER stress pathway on the inflammatory reactions observed in the livers of HFD-fed mice, we analyzed mRNA expression of ER stress- related genes: binding immunoglobulin protein (BiP), X-box-binding protein (XBP-1), activating transcription factor 4 (ATF4), activating transcription factor 6 (ATF6), and C/EBP homologous protein (CHOP) in the livers of ND- and HD-fed mice. There were no differences in mRNA expression levels of ATF4 and ATF6 between ND, HFD4, and HFD14. However, mRNA levels of BiP in HFD4, and CHOP in HFD4 and HFD14 significantly increased, and that of XBP-1 in HFD14 significantly decreased, compared with those in ND-mice ($p<0.05$, respectively), indicating the induction of ER stress responses with short-term HFD intake. The decrease of XBP-1 mRNA levels during HFD intake implies the downregulation of ER associated degradation (ERAD) mechanism that reduces ER

stress, conversely meaning the increase of ER stress. And the increase of CHOP mRNA levels suggests the increase of not only ER stress but also susceptibility to apoptosis of hepatocytes (Fig. 2). We also examined mRNA expression of the genes related to hypoxia and oxidative

stress responses. To evaluate hypoxia response which is possibly induced by acceleration of mitochondrial aerobic metabolism [23], we examined mRNA levels of hypoxia- inducible factor-1α (HIF-1α). But we could not find difference in the HIF-1α mRNA levels between ND and HFD-fed mice. mRNA levels of heme oxygenase-1 (HO-1) and Mn-superoxide dismutase (MnSOD) were examined to assess oxidative stress response in the liver. HO-1 mRNA levels were not different between ND- and HFD-fed mice, but MnSOD mRNA levels were significantly lower in HFD14 mice than in ND mice ($p<0.05$). It has been reported that expression of MnSOD mRNA is negatively correlated with increased hepatic fat storage in the male mice [24], and our results seems consistent with this report (Fig. 2).

We observed the induction of ER stress response and decrease of MnSOD expression in the liver of mice fed with short-term HFD. However, 8-OHdG immunostaining of these liver tissues did not show positive staining areas except for the necro-inflammatory lesions caused by Con A administration, even in HFD-fed mice (Suppl Fig. 1).

5. Influence of HFD feeding on the severity of Con A-induced liver injury

Next, we compared severity of Con A-induced liver injury between ND- and HFD- fed mice. In ND mice, serum ALT levels 24 hour after Con A administration was 302 ± 227 U/l. In HFD4 and HFD14 mice, ALT levels were 4675 ± 2211 U/l and 3950 ± 2210 U/l, respectively, both showing significant elevation compared with those of ND mice ($p<0.05$, respectively, Fig. 3B, Suppl Table 1).

In histological analysis, relatively small, scattered necro-inflammatory lesions were found in ND mice, while larger necro-inflammatory lesions were extensively observed in HFD4 and HFD14 mice (Fig. 3C). The extent of liver damage in the histology did not differ between HFD4 and HFD14 mice consistent with the ALT levels.

The immunostaining for fibrinogen/fibrin showed the deposition of fibrinogen/fibrin in the areas almost consistent with widespread necro-inflammatory lesions, both in HFD4 and HFD14 mice. In ND mice, small necro-inflammatory lesions and liver sinusoids in the lobules were positive for the staining (Fig. 3D).

6. Kinetics of hepatic mRNA expression patterns in the early phase of Con A-induced liver injury

Serial changes in ALT levels, liver histology, and hepatic mRNA expression patterns in ND and HFD4 mice were investigated 1 and 3 h after Con A administration (Fig. 4A), since the hepatic inflammatory reactions in this time period have been known to determine the magnitude of liver injury in this model [15]. Serum ALT levels and liver histology showed no significant changes in both groups during the observation period up to 3 h, although marked elevation of ALT levels and wide-spread necro-inflammatory lesions were observed at 24 h after Con A administration only in

HFD4 mice (Fig. 4B, 4C), consistent with the results in the former experiment. In the analysis for hepatic mRNA expression levels of cytokines/chemokines, those of IFN-γ, IL-1α, IL-6, IL-10 peaked at 1 h after Con A administration, while those of TNF-α and MCP-1 increased over time until 3 h after Con A administration (Fig. 4D). mRNA expression patterns of cell surface markers suggested increased migration of monocytes/macrophages, NK cells, and neutrophils, but decrease of KCs in HFD4 mice. There were no apparent differences in mRNA expression patterns of cytokines/chemokines and cell surface markers between ND and HFD4 mice, except for those of F4/80 which showed continuous decrease in HFD4 mice and no apparent change in ND mice (Fig. 4D).

mRNA levels of coagulation-related molecules increased over time until 3 h after Con A administration in both group of mice. They also showed no marked differences between the two groups, except for TF mRNA levels. Namely, TF mRNA levels at 3 h after Con A administration were significantly higher in HFD4 than in ND ($p<0.05$, Fig. 4D).

There were also no big differences in mRNA expression patterns of ER stress-, hypoxia-, and oxidative stress-related genes between ND and HFD4 mice. The elevation of BiP, XBP-1, CHOP, HO-1, and MnSOD mRNA levels suggested the existence of ER and oxidative stresses induced by Con A administration.

7. Heparin treatment against the Con A-induced liver injury

Then, we pretreated mice with heparin prior to Con A administration to examine how hypercoagulability is related to the severity of liver injury. In ND mice, ALT levels 24 h after Con A administration were significantly decreased in heparin-treated mice (36 ± 9 U/l) compared with non-treated mice (434 ± 175 U/l, $p<0.05$). In HFD4 mice, ALT levels 24 h after Con A administration showed more significant decline by heparin treatment: non-treated mice, 5934 ± 2706 U/l; heparin-treated mice, 112 ± 78 U/l ($p<0.05$). ALT levels 24 h after Con A administration in the mice with heparin treatment still tended to be higher in HFD4 mice than in ND mice ($p=0.059$, Fig. 5A, 5B, Suppl Table 1). In ND mice, the liver histology in heparin-treated mice showed significant improvement in inflammation, without apparent necro-inflammatory lesions and degenerated hepatocytes. In HFD4 mice, the extent of improvement in liver histology by the heparin treatment was more prominent than that in ND mice. In heparin-treated HFD4 mice, widespread necro- inflammatory lesions were almost disappeared, but scattered degenerated hepatocytes were observed consistent with the slightly elevated ALT levels (Fig. 5C).

In the analysis of hepatic mRNA expression patterns of the mice before Con A administration, heparin treatment did not affect mRNA expression levels of most of the cytokine/chemokine, coagulation- and ER stress-related genes both in ND and HFD4 mice. There were only two exceptions: TNF-α mRNA levels in HFD4 mice showed slight but significant elevation, and XBP-1 mRNA in ND mice showed significant decline by the heparin treatment ($p<0.05$, respectively). Most of other changes in mRNA levels were associated with liver injury by Con A administration or amelioration of Con A-induced liver injury by the heparin treatment (Supple Fig. 2).

Fibrinogen/fibrin immunostaining for the liver tissues of heparin-treated mice 24 h after Con A

administration, showed strong deposition of fibrinogen/fibrin in the sinusoids both in ND and HFD4 mice. Considering the increase of Fbg-α mRNA levels by Con A administration and efficient inhibition of clot formation of fibrin by heparin treatment, it is strongly suggested that the deposition detected in the sinusoids was fibrinogen, not fibrin clot (Fig. 5D).

Discussion

In the current study, we indicated that just short-term HFD intake for just 4 days, caused proinflammatory and procoagulation states in the livers of mice.

As described, Cleuren et al. have reported that HFD intake for 14 days induces increase of plasma levels of inflammatory cytokines and coagulation factors in mice, while the mechanism for this is not clearly elucidated [5]. It has also been reported that HFD intake for 3 days can induces activation of inflammatory/immune pathways in mice livers which are mainly controlled by nuclear factor-κB (NFκB) signaling [25]. Since the close relationship between inflammatory cytokines and coagulation-related factors, such as TF, has been reported [20,26,27], we thought that HFD-induced NFκB activation lead to the development of proinflammatory state and subsequently to the development of procoagulation state.

In the analysis of gene expressions related to glucose metabolism, we observed the suppression of PDK4 mRNA level by HFD intake (Fig. 2), which suggests the increase of acetyl-CoA production and the acceleration of aerobic metabolic pathway, usually leading to the increased production of reactive oxygen species (ROS) in mitochondria [28]. It has also been reported that hyperglycemia or hyperlipidemia themselves induce mitochondrial ROS production [29,30]. Since ROS is known to activate ER stress pathways, or directly induce inflammatory cytokines, such as TNF-α [28,31], it may also explain the mechanism that induced proinflammatory state in HFD-fed mice in the current study.

It is recently reported that the transition of diet consumption between fasting and feeding immediately induces ER stress responses in the liver of mice [32]. While we cannot clarify the relevance of the report to our findings, we observed the increase of BiP and CHOP mRNA levels the liver of HFD-fed mice, which indicates the presence of ER stress responses (Fig. 2). We expected the activation of inositol requiring 1 (IRE1) pathway, one of the major ER stress pathways which is known to activate NFκB signaling, but we could not indicate the direct evidence for that in the current study. We also expected the involvement of hypoxia- and oxidative stress-related factors in the induction of inflammatory responses during short-term HFD, but we could not show the significant changes in mRNA expression of these factors (Fig. 2). In 8-OHdG immunostaining, no apparent oxidative DNA damage were detected in HFD-fed mice with or without Con A administration, except in the necrotic lesions in Con A administered-mice (Suppl Fig. 1). These suggest that the cellular stresses induced by short-term HFD were enough to provoke inflammatory responses in the liver, but not enough to cause apparent oxidative damage to the liver cells. Since the involvement of cellular stresses is the feature of NASH pathogenesis and the current study showed the induction of hepatic cellular stresses after Con A administration, it is required to investigate the relationship between duration of HFD diet and induction of cellular stresses.

We observed the increase of IFN-γ and IL-10 mRNA expression as well as those of TNF-a and MCP-1 in the liver of HFD-fed mice (Fig. 2). We assumed the involvement of NFκB signaling pathways in hepatocytes for the induction of proinflammatory states in the short-term HFD loading, but at least IFN-γ is not produced by hepatocytes. The current study suggested the increase of monocytes, NK cells, and neutrophils, and the expansion of KCs in the livers of HFD-fed mice.

There are many inflammatory stimuli circulating to the liver, such as lipopolysaccharide and secondary bile acids, which are the candidates of so-called “second hits” as suggested in NASH pathogenesis. Therefore, it is thought that these “second hits” stimulate liver-resident KCs, LSECs, HSCs, and DCs to produce cytokines and chemokines, causing activation of immune cells, some of which produced IFN-γ. Moreover, it has also been reported that the functions of KCs, LSECs, and HSCs are modulated directly by HFD loading and that these modulations possibly contribute the development of NASH [17,33,34]. The exact mechanism for the induction of proinflammatory state by HFD need to be elucidated in detail in the further study. Importantly, we indicated that severity of Con A-induced liver injury was greatly exacerbated with short-term (for 4 days) HFD intake even in the absence of obvious fatty liver in the mouse model (Fig. 1C).

In the Con A-induced liver injury model, it has been reported that IFN-γ and TNF-α mainly produced from Con A-stimulated T cells facilitate the production of TF and PAI-1, resulting in the induction of procoagulation state, and that subsequent thrombus formation in sinusoids causes extensive liver necrosis [15]. Con A-induced liver injury is considered as a model of autoimmune hepatitis, but thrombus formation subsequent to the liver damage, is recognized as a common pathology of severe liver injury [35]. Indeed, it has been proven that the deposition of fibrin as intravascular microthrombi obstruct local hepatic blood flow causing extended liver damage in many of the liver injury model [36,37].

We observed increased deposition of fibrinogen in the liver sinusoids in HFD-fed mice without the increase of plasma levels and hepatic mRNA expression levels of fibrinogen (Fig. 1C, Fig. 2, Table 3). It has been reported in the human study that even single HFD causes the decrease of flow mediated vasodilation inversely proportional to the serum TG levels, and that saturated fatty acids induce an increased expression of the proinflammatory adhesion molecules, such as intercellular adhesion molecule-1 (ICAM-1) and vascular cell adhesion molecule-1 (VCAM-1) on epithelial cells [38]. It has also been reported that 6 to 10 weeks of choline deficient, amino-acid defined HFD enhances expression of integrin α5β1 [39], a ligand of fibrinogen [40]. Therefore, it is speculated that HFD causes the disturbance of blood flow in liver sinusoids and the enhancement of integrin expression including α5β1, resulting in the increased deposition of fibrinogen in sinusoids. The results of immunostaining of fibrinogen/fibrin in the Con A-administered mice suggests that the deposition of fibrinogen/fibrin were increased by inflammation, probably through the enhanced expression of fibrinogen and integrins on LSECs (Fig. 5D). From the results in the current study, we believe that the deposition of fibrinogen together with the increase of TF and PAI-1 expression induced by short-term HFD played the significant role in the exacerbation of liver injury. However, the mechanism of fibrinogen deposition in sinusoids, especially the involvement of LSECs, should be further examined in detail to clarify the risk of HFD.

Since the dose of Con A administered to mice in the current experiment was the half of the usual experiment, the extent of liver injury was relatively low compared to the reports dealing with Con A liver injury model. But it was amplified about ten times in ALT levels by the short-term HFD intake. We think this partly implies the possible mechanism for the development of NASH as suggested in “multiple parallel hits theory” [8]. Namely, diet-related oxidative stress, production

of ROS, and ER stress may cause proinflammatory and procoagulation states in the liver, and increase the susceptibility of hepatocytes against many inflammatory stimuli circulating to the liver, like lipopolysaccharide and secondary bile acids, produced or metabolized by gut microbes. Along with the progression of hepatic triglyceride accumulation or steatosis, these may cooperatively cause progressive inflammatory and fibrotic change in the liver, finally leading to the development of NASH.

To prove the hypothesis above, we should consider examining the susceptibility to liver injury in the HFD-fed mice using more physiological stimuli, such as lipopolysaccharide. The influence of HFD intake in a wider range of duration should also be evaluated, referring the report about the transition of hepatic mRNA expression patterns during HFD feeding [25]. Furthermore, the influence of HFD intake in other background of mice should be examined to evaluate the relevance of genetic factors, as the relevance of genetic background to the development of NASH is reported in human study [41,42].

In the current study, we reported that just short-term HFD intake increased the susceptibility of the liver to inflammatory stimuli through the induction of procoagulation state in the livers of mice. We think that it explains a part of NASH pathogenesis, and appears to support the previously reported effects of anticoagulant therapy on NAFLD and NASH [43,44].

Acknowledgement

Authors thank Ms. Kanako Yamazaki, Ai Imaida, Machi Yamamoto, Hiroko Suzuki, Airi Ishikawa, Mr. Ryo Iwase, Yasuhiro Takizaki, and Hiroyuki Takimoto for technical assistance and helpful discussions. This work is partly supported by the grant from Merck Sharp & Dohme K. K., Tokyo, Japan (No. 6100030047).

References

1. Ellulu MS, Patimah I, Khaza'ai H, Rahmat A, Abed Y, Obesity and inflammation: the linkingmechanism and the complications, Arch Med Sci. 13 (2017) 851-863
2. Mertens I, Van Gaal LF, Obesity, haemostasis and the fibrinolytic system, Obes Rev. 3 (2002) 85-101
3. Samad F, Ruf W, Inflammation, obesity, and thrombosis, Blood. 122 (2013) 3415-22
4. Hariri N, Thibault L, High-fat diet-induced obesity in animal models, Nutr Res Rev. 23 (2010) 270-99
5. Cleuren AC, Blankevoort VT, van Diepen JA, Verhoef D, Voshol PJ, Reitsma PH, van Vlijmen BJ, Changes in dietary fat content rapidly alters the mouse plasma coagulation pofile without affecting relative transcript levels of coagulation factors, PLoS One. 10 (2015) e0131859
6. Milić S, Lulić D, Štimac D, Non-alcoholic fatty liver disease and obesity: biochemical, metabolic and clinical presentations, World J Gastroenterol. 20 (2014) 9330-7
7. Dowman JK, Tomlinson JW, Newsome PN, Pathogenesis of non-alcoholic fatty liver disease, QJM. 103 (2010) 71-83
8. Buzzetti E, Pinzani M, Tsochatzis EA, The multiple-hit pathogenesis of non-alcoholic fatty liver disease (NAFLD), Metabolism. 65 (2016) 1038-48
9. Tiegs G, Hentschel J, Wendel A, A T cell-dependent experimental liver injury in mice inducible by concanavalin A, J Clin Invest. 90 (1992) 196-203
10. Gantner F, Leist M, Lohse AW, Germann PG, Tiegs G, Concanavalin A-induced T- cell-mediated hepatic injury in mice: the role of tumor necrosis factor, Hepatology. 21 (1995) 190-8
11. Takeda K, Hayakawa Y, Van Kaer L, Matsuda H, Yagita H, Okumura K, Critical contribution of liver natural killer T cells to a murine model of hepatitis, Proc Natl Acad Sci U S A. 97 (2000) 5498-503
12. Heymann F, Hamesch K, Weiskirchen R, Tacke F, The concanavalin A model of acute hepatitis in mice, Lab Anim. 49 (1 Suppl) (2015) 12-20
13. Rani R, Tandon A, Wang J, Kumar S, Gandhi CR, Stellate cells orchestrate concanavalin A-induced acute liver damage, Am J Pathol. 187 (2017) 2008-2019
14. Rani R, Kumar S, Sharma A, Mohanty SK, Donnelly B, Tiao GM, Gandhi CR, Mechanisms of concanavalin A-induced cytokine synthesis by hepatic stellate cells: distinct roles of interferon regulatory factor-1 in liver injury, J Biol Chem. 293 (2018) 18466-18476
15. Kato J, Okamoto T, Motoyama H, Uchiyama R, Kirchhofer D, Van Rooijen N, Enomoto H, Nishiguchi S, Kawada N, Fujimoto J, Tsutsui H, Interferon-gamma-mediated tissue factor expression contributes to T-cell-mediated hepatitis through induction of hypercoagulation in mice, Hepatology. 57 (2013) 362-72
16. Narayanan S, Surette FA, Hahn YS, The immune landscape in nonalcoholic steatohepatitis. Immune Netw. 16 (2016) 147–158
17. Hammoutene A, Rautou PE, Role of liver sinusoidal endothelial cells in non-alcoholic fatty liver disease, J Hepatol. 70 (2019) 1278-1291

18. Majer M, Popov KM, Harris RA, Bogardus C, Prochazka M. Insulin downregulates pyruvate dehydrogenase kinase (PDK) mRNA: potential mechanism contributing to increased lipid oxidation in insulin-resistant subjects. Mol Genet Metab. 65 (1998) 181-6.
19. Park S, Jeon JH, Min BK, Ha CM, Thoudam T, Park BY, Lee IK, Role of the pyruvate dehydrogenase complex in metabolic remodeling: differential pyruvate dehydrogenase complex functions in metabolism, Diabetes Metab J. 42 (2018) 270-81
20. Faber DR, Kalkhoven E, Westerink J, Bouwman JJ, Monajemi HM, Visseren FL, Conditioned media from (pre)adipocytes stimulate fibrinogen and PAI-1 production by HepG2 hepatoma cells, Nutr Diabetes. 3 (2012) e52
21. Redman CM, Xia H, Fibrinogen biosynthesis. Assembly, intracellular degradation, and association with lipid synthesis and secretion, Ann N Y Acad Sci. 936 (2001) 480-95
22. Puri P, Mirshahi F, Cheung O, Natarajan R, Maher JW, Kellum JM, Sanyal AJ, Activation and dysregulation of the unfolded protein response in nonalcoholic fatty liver disease, Gastroenterology. 134 (2008) 568-76
23. Solaini G, Baracca A, Lenaz G, Sgarbi G, Hypoxia and mitochondrial oxidative metabolism, Biochim Biophys Acta. 1797 (2010) 1171-7
24. Krautbauer S, Eisinger K, Lupke M, Wanninger J, Ruemmele P, Hader Y, Weiss TS, Buechler C, Manganese superoxide dismutase is reduced in the liver of male but not female humans and rodents with non-alcoholic fatty liver disease, Exp Mol Pathol. 95 (2013) 330- 5
25. Radonjic M, de Haan JR, van Erk MJ, van Dijk KW, van den Berg SA, de Groot PJ, Müller M, van Ommen B, Genome-wide mRNA expression analysis of hepatic adaptation to high-fat diets reveals switch from an inflammatory to steatotic transcriptional program, PLoS One. 4 (2009) e6646.
26. Grignani G, Maiolo A, Cytokines and hemostasis, Haematologica. 85 (2000) 967-72
27. Foley JH, Conway EM, Cross talk pathways between coagulation and inflammation, Circ Res, 118 (2016) 1392-408
28. Forrester SJ, Kikuchi DS, Hernandes MS, Xu Q, Griendling KK, Reactive oxygen species in metabolic and inflammatory signaling. Circ Res. 122 (2018) 877-902
29. Sada K, Nishikawa T, Kukidome D, Yoshinaga T, Kajihara N, Sonoda K, Senokuchi T, Motoshima H, Matsumura T, Araki E, Hyperglycemia induces cellular hypoxia through production of mitochondrial ROS followed by suppression of Aquaporin-1, PLoS One. 11 (2016) e0158619
30. Amiya E, Interaction of hyperlipidemia and reactive oxygen species: Insights from the lipid-raft platform, World J Cardiol. 8 (2016) 689-94
31. Bulua AC, Simon A, Maddipati R, Pelletier M, Park H, Kim KY, Sack MN, Kastner DL, Siegel RM, Mitochondrial reactive oxygen species promote production of proinflammatory cytokines and are elevated in TNFR1-associated periodic syndrome (TRAPS), J Exp Med. 208 (2011) 519-33
32. Sasako T, Ohsugi M, Kubota N, Itoh S, Okazaki Y, Terai A, Kubota T, Yamashita S, Nakatsukasa K, Kamura T, Iwayama K, Tokuyama K, Kiyonari H, Furuta Y, Shibahara J,

Fukayama M, Enooku K, Okushin K, Tsutsumi T, Tateishi R, Tobe K, Asahara H, Koike K, Kadowaki T, Ueki K, Hepatic Sdf2l1 controls feeding-induced ER stress and regulates metabolism, Nat Commun. 10 (2019) 947

33. McGettigan B, McMahan R, Orlicky D, Burchill M, Danhorn T, Francis P, Cheng LL, Golden-Mason L, Jakubzick CV, Rosen HR, Dietary lipids differentially shape nonalcoholic steatohepatitis progression and the transcriptome of Kupffer cells and infiltrating macrophages, Hepatology. 70 (2019) 67-83
34. Barbero-Becerra VJ, Giraudi PJ, Chávez-Tapia NC, Uribe M, Tiribelli C, Rosso N, The interplay between hepatic stellate cells and hepatocytes in an in vitro model of NASH, Toxicol In Vitro. 29 (2015) 1753-8
35. Northup PG, Sundaram V, Fallon MB, Reddy KR, Balogun RA, Sanyal AJ, Anstee QM, Hoffman MR, Ikura Y, Caldwell SH; Coagulation in Liver Disease Group, Hypercoagulation and thrombophilia in liver disease, J Thromb Haemost. 6 (2008) 2-9
36. Fujiwara K, Ogata I, Ohta Y, Hirata K, Oka Y, Yamada S, Sato Y, Masaki N, Oka H, Intravascular coagulation in acute liver failure in rats and its treatment with antithrombin III, Gut. 29 (1988) 1103-8
37. Rautou PE, Tatsumi K, Antoniak S, Owens AP, Sparkenbaugh E, Holle LA, Wolberg AS, Kopec AK, Pawlinski R, Luyendyk JP, Mackman N, Hepatocyte tissue factor contributes to the hypercoagulable state in a mouse model of chronic liver injury, J Hepatol. 64 (2016) 53-9
38. Yucel N, Arany Z, Fat, obesity, and the endothelium, Curr Opin in Physiol. 12 (2019) 44–50
39. Ulmasov B, Noritake H, Carmichael P, Oshima K, Griggs DW, Neuschwander-Tetri BA, An inhibitor of arginine-glycine-aspartate-binding integrins reverses fibrosis in a mouse model of nonalcoholic steatohepatitis, Hepatol Commun. 3 (2018) 246-261
40. Suehiro K, Gailit J, Plow EF, Fibrinogen is a ligand for integrin alpha5beta1 on endothelial cells, J Biol Chem. 272 (1997) 5360-6.
41. Romeo S, Kozlitina J, Xing C, Pertsemlidis A, Cox D, Pennacchio LA, Boerwinkle E, Cohen JC, Hobbs HH, Genetic variation in PNPLA3 confers susceptibility to nonalcoholic fatty liver disease. Nat Genet. 40 (2008) 1461-5
42. Liu YL, Reeves HL, Burt AD, Tiniakos D, McPherson S, Leathart JB, Allison ME, Alexander GJ, Piguet AC, Anty R, Donaldson P, Aithal GP, Francque S, Van Gaal L, Clement K, Ratziu V, Dufour JF, Day CP, Daly AK, Anstee QM, TM6SF2 rs58542926 influences hepatic fibrosis progression in patients with non-alcoholic fatty liver disease. Nat Commun. 5 (2014) 4309
43. Kopec AK, Joshi N, Towery KL, Kassel KM, Sullivan BP, Flick MJ, Luyendyk JP, Thrombin inhibition with dabigatran protects against high-fat diet-induced fatty liver disease in mice, J Pharmacol Exp Ther. 351 (2014) 288-97
44. Lisman T, Jenne CN, Fibrin fuels fatty liver disease. J Thromb Haemost, 16 (2019) 3– 5

Figure legends

Figure.1 Serum biochemistry and liver histology.

(A) Experimental scheme. ND: the mice fed with ND, HFD1, HFD2, HFD4 and HFD14: the mice fed with HFD for 1 day, 2 days, 4 days and 14 days, respectively.

(B) The results of serum ALT (U/l), total cholesterol (T-Cho, mg/dl), triglyceride (TG, mg/dl), and glucose (Glu, mg/dl). The data are shown as means ± SD. * $p<0.05$.

(C) H&E and fibrin/fibrinogen immunostaining of representative liver sections from the individual groups of mice. In each group, the left column shows H&E-staining and the right column shows fibrin/fibrinogen immunostaining. 4x objective's scale bar: 200μm. 10x objective's scale bar: 50μm. 20x objective's scale bar: 20μm.

(D) Oil Red O staining of representative liver sections from the individual groups of mice. 4x objective's scale bar: 200μm. 10x objective's scale bar: 50μm. 20x objective's scale bar: 20μm.

Figure.2 Hepatic mRNA expression.

Intrahepatic mRNA expression levels were measured by qRT-PCR. Expression levels of the respective mRNAs are normalized to that of GAPDH and normalized data are presented as fold change compared with ND-fed mice. The data are shown as means ± SD. * $P<0.05$ vs. ND-fed mice.

Figure.3 Extent of Con A-induced liver injury.

(A) Experimental scheme.

(B) Serum ALT levels 24 h after Con A administration. The data are shown as means ± SD (U/l). * $p<0.05$.

(C) H&E staining of representative liver sections. From left to right, ND mice without Con A administration, ND, HFD4, and HFD14 mice, 24 h after Con A administration, respectively. 4x objective's scale bar: 200μm. 10x objective's scale bar: 50μm.

(D) Fibrin/fibrinogen immunostaining of serial liver sections from the same mice as (C). 4x objective's scale bar: 200μm. 10x objective's scale bar: 50μm. 20x objective's scale bar: 20μm.

Figure.4 Sequential changes of serum ALT levels, histology and hepatic mRNA expressions in ND and HFD-fed mice in the early phase of Con A-induced liver injury.

(A) Experimental scheme.

(B) The results of serum ALT (U/l). * $p<0.05$.

(C) H&E staining of representative liver sections. Left panel shows the histology of ND mice and right panel shows that of HFD4 mice. In each panel, from left to right, histology of the mice with 1 h, 3 h, or 24 h after Con A administration, respectively. 4x objective's scale bar: 200μm. 10x objective's scale bar: 50μm.

(D) Intrahepatic mRNA expression levels measured by qRT-PCR. * $p<0.05$.

Figure.5 Therapeutic effect of heparin on Con A-induced liver injury.

(A) Experimental scheme.

(B) Serum ALT levels 24 h after Con A administration with or without heparin in ND and HFD4 mice. The data are shown as means ± SD (U/l). * $p<0.05$.

(C) H&E staining of representative liver sections from the individual groups of mice 24 h after Con A administration. From left to right, ND mice, ND mice with heparin, HFD4 mice, and HFD4 mice with heparin, respectively. Arrow heads indicate degenerated hepatocytes (HFD4 mice with heparin). 4x objective's scale bar: 200μm. 10x objective's scale bar: 50μm. 20x objective's scale bar: 20μm.

(D) Fibrin/fibrinogen immunostaining of serial liver sections from the same mice as (C). 10x objective's scale bar: 50μm. 20x objective's scale bar: 20μm.

Figure1

(A)

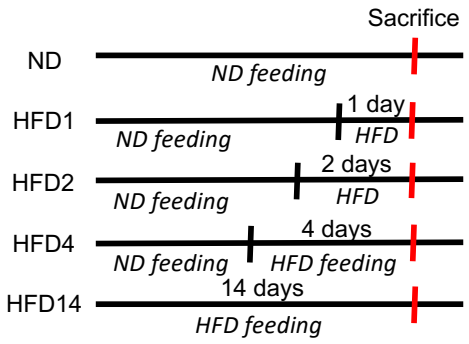

(B)

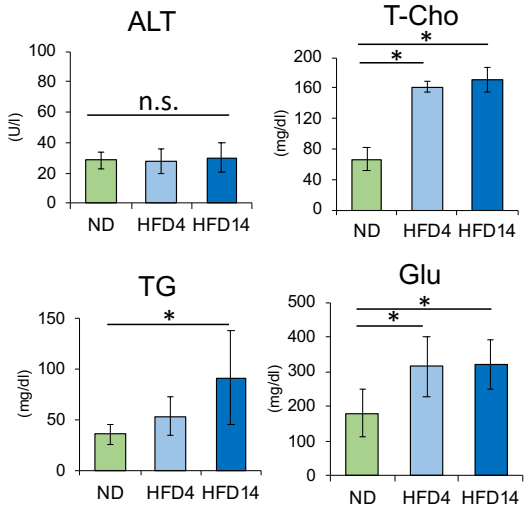

(C)

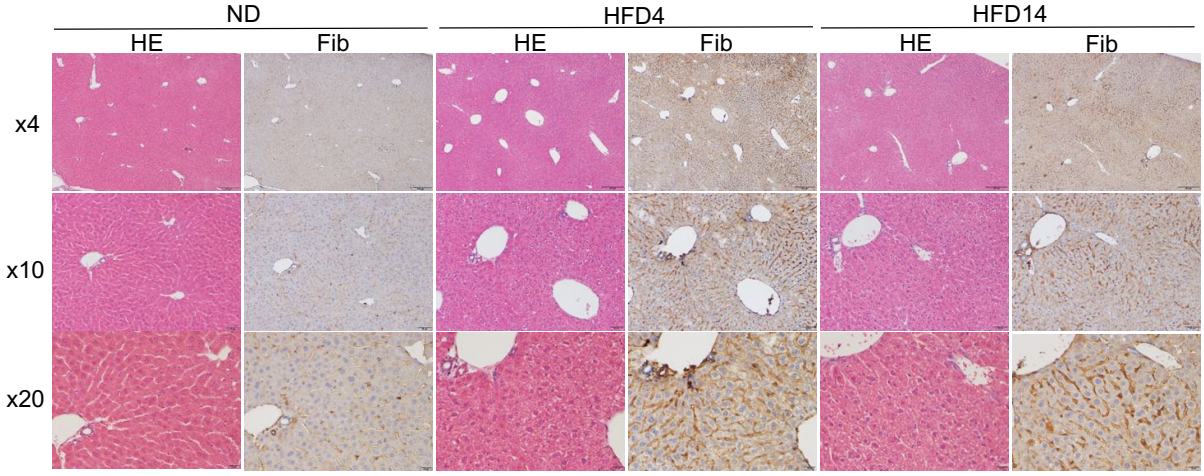

(D)

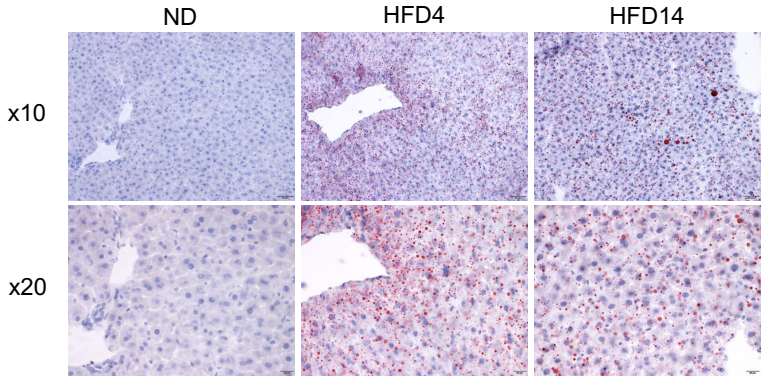

Figure.2

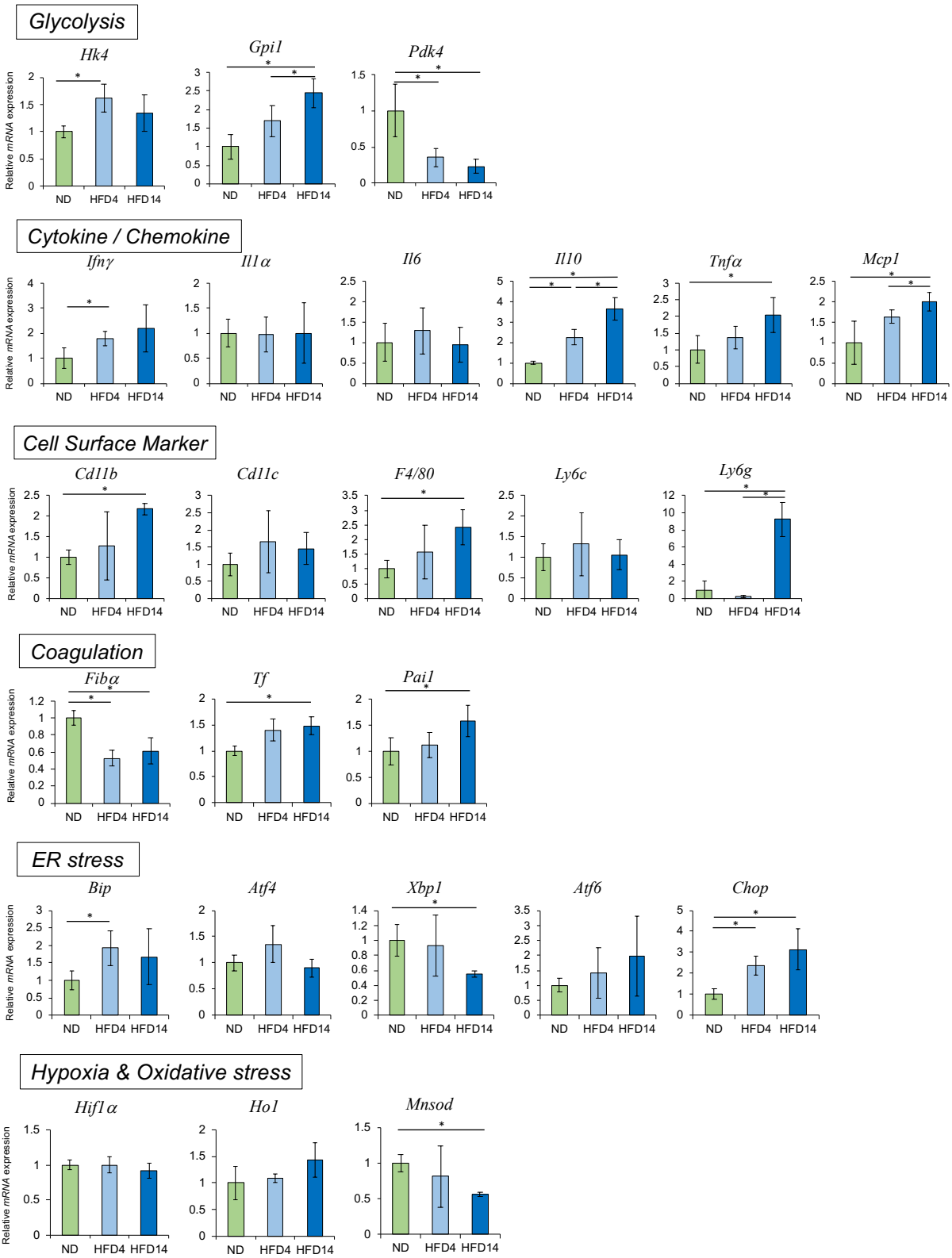
Glycolysis
Hk4
Gpi1
Pdk4
Cytokine / Chemokine
Ifnγ
Il1α
Il6
Il10
Tnfα
Mcp1
Cell Surface Marker
Cd11b
Cd11c
F4/80
Ly6c
Ly6g
Coagulation
Fibα
Tf
Pai1
ER stress
Bip
Atf4
Xbp1
Atf6
Chop
Hypoxia & Oxidative stress
Hif1α
Ho1
Mnsod
Relative mRNA expression
ND
HFD4
HFD14

Figure.3

(A)

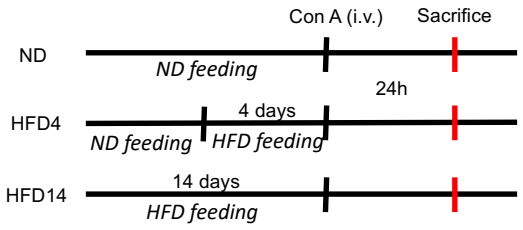

(B)

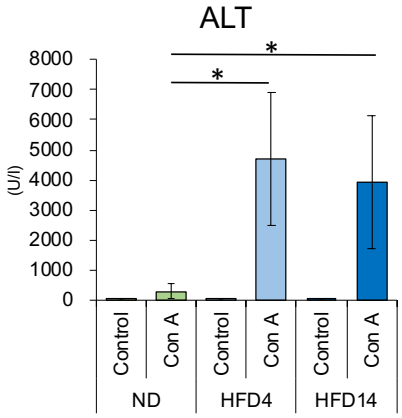

(C)

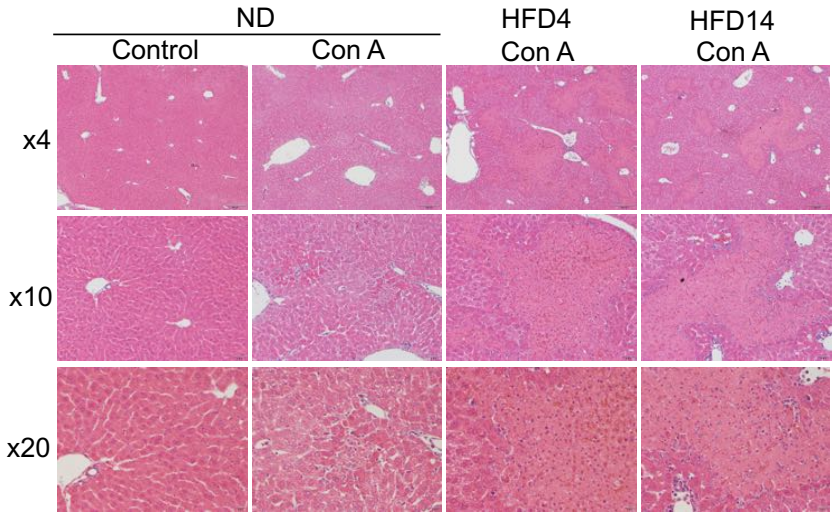

(D)

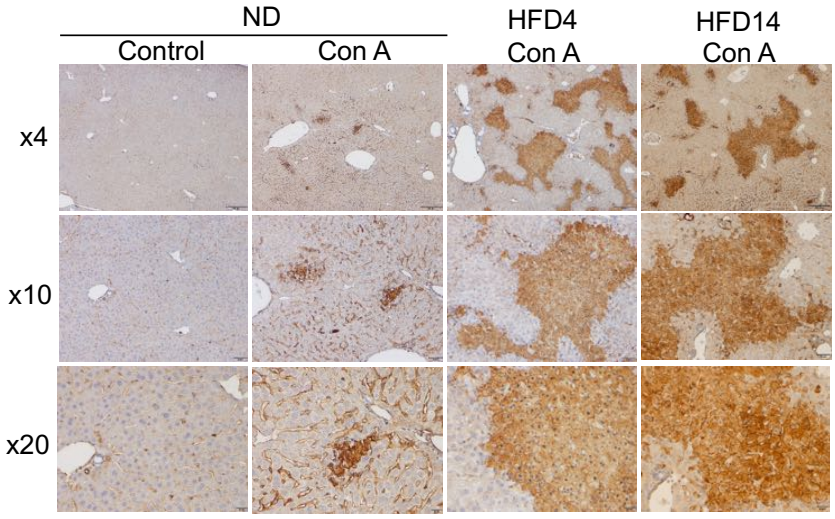

Figure. 4

(A)

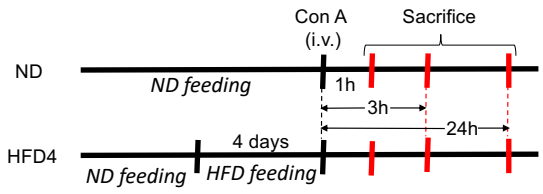

(B)

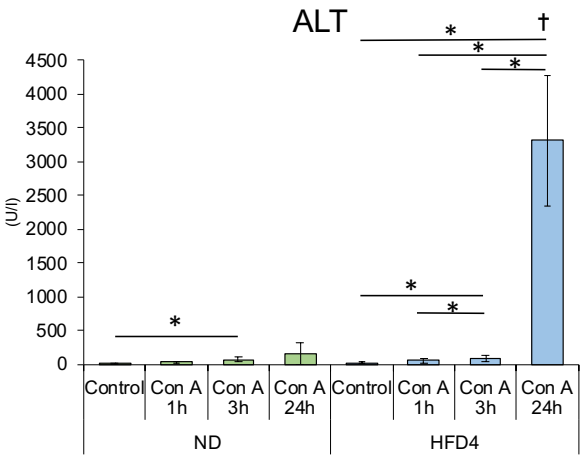

(C)

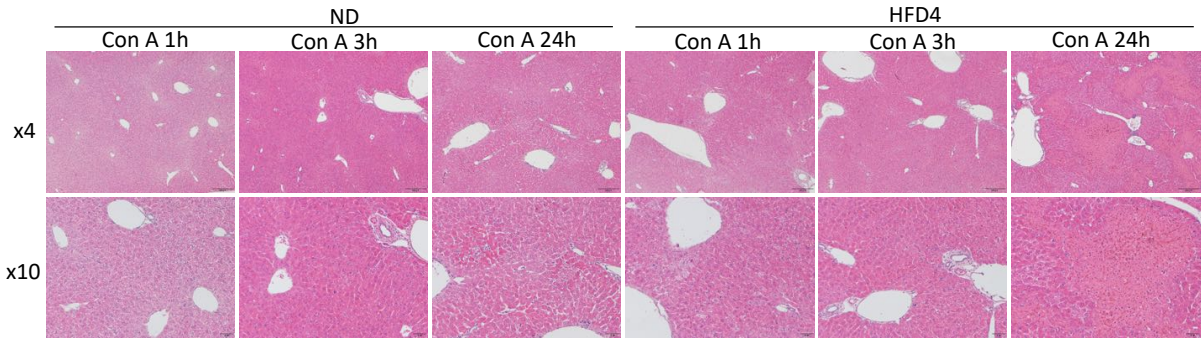

(D)

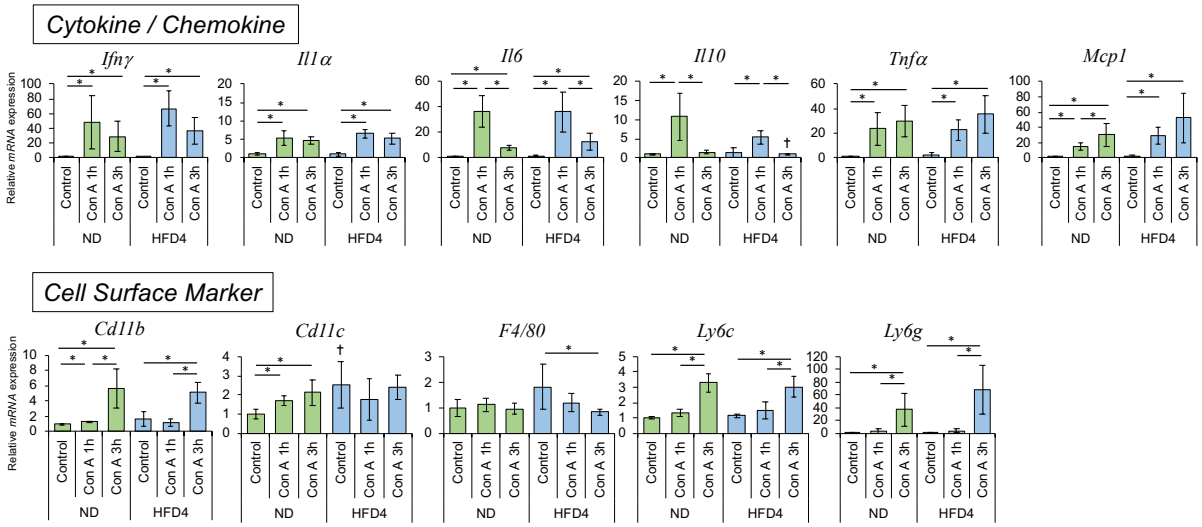

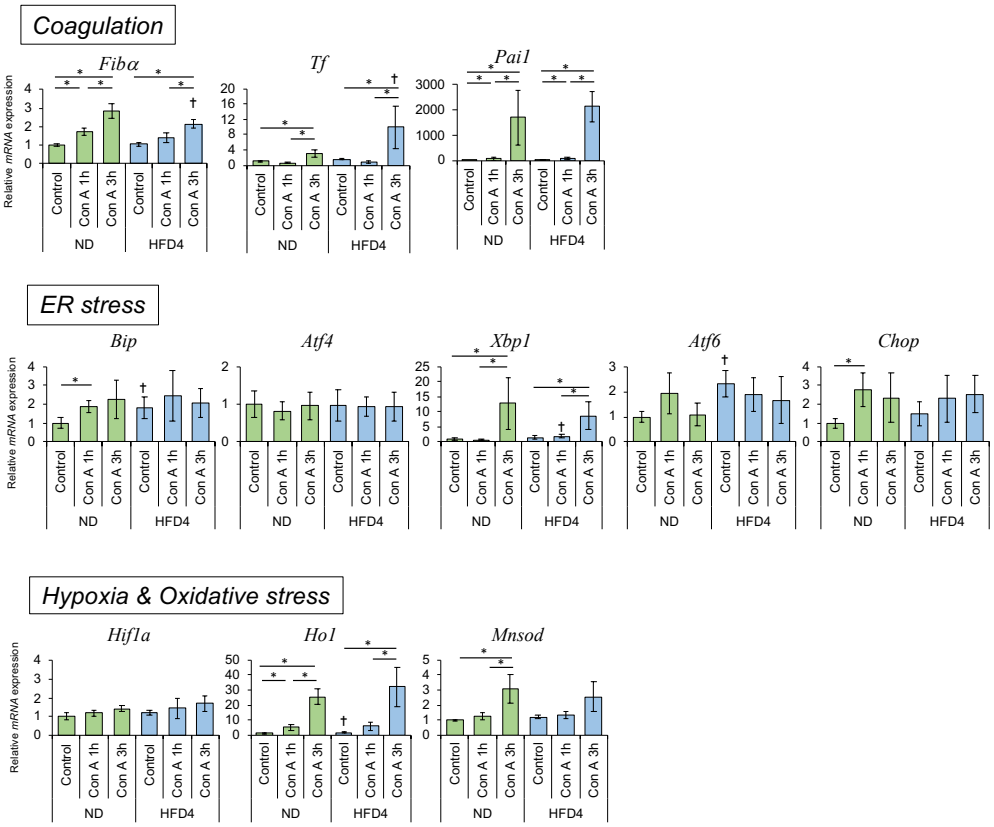
Coagulation
Fibα
Tf
Pai1
ER stress
Bip
Atf4
Xbp1
Atf6
Chop
Hypoxia & Oxidative stress
Hif1a
Ho1
Mnsod
Relative mRNA expression
Control
Con A 1h
Con A 3h
ND
HFD4

Figure5.

(A)

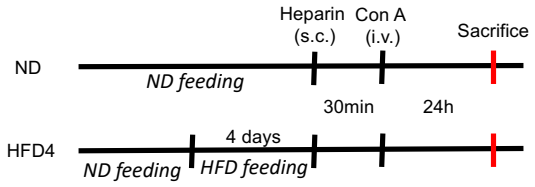

(B)

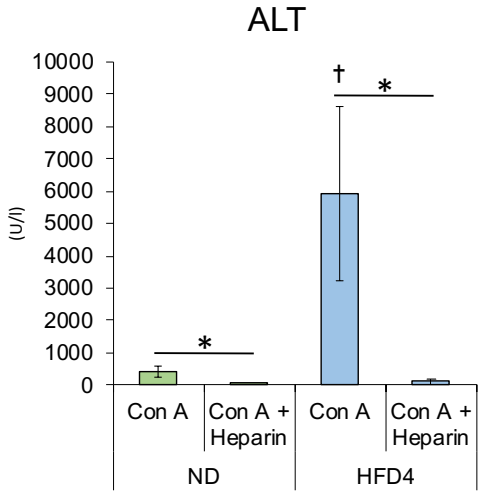

(C)

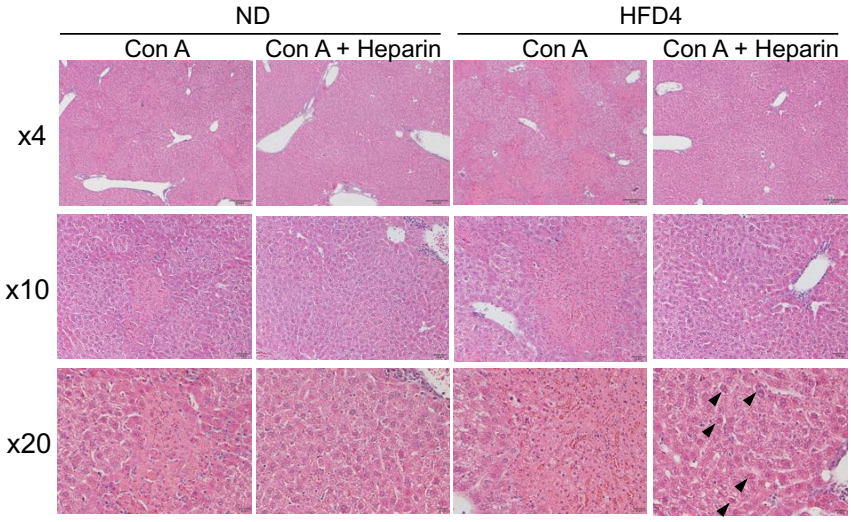

(D)

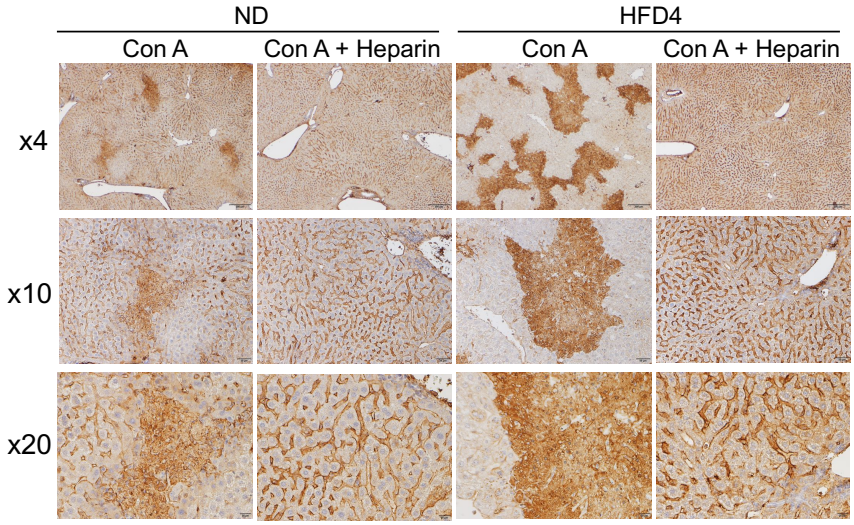

Nutritional composition	CE2	High Fat Diet 32
(per 100g diet)	(ND: normal diet)	(HFD: high fat diet)
Moisture (%)	8.84	6.2
Crude protein (%)	25.48	25.5
Crude fat (%)	4.61	32
Crude fiber (%)	5.14	2.9
Crude ash (%)	7.01	4
Nitrogen free extract (NFE) (%)	48.92	29.4
Energy (kcal)	339.1	507.6

Table 1 Diet compositions of normal diet (ND) and high-fat diet (HFD).

Gene	Forward primer sequences (5'--3')	Reverse primer sequences (5'--3')
Gapdh	TGTGTCCGTCGTGGATCTGA	TTGCTGTTGAAGTCGCAGGAG
Hk4	CATCCTGCTCAACTGGACCAA	CATTGCCACCACATCCATCTC
Gpi1	GTGGTCAGCCATTGGACTTT	CTTTCCGTTGGACTCCATGT
Pdk4	AGTGACTCAAAGACGGGAAAC	GTGTGAGGTTTAATTCTGGCG
Ifng	CGGCACAGTCATTGAAAGCCTA	GTTGCTGATGGCCTGATTGTC
Il1a	TGGTTAAATGACCTGCAACAGGAA	AGGTCGGTCTCACTACCTGTGATG
Il6	CCACTTCACAAGTCGGAGGCTTA	CCAGTTTGGTAGCATCCATCATTTC
Il10	GCCAGAGCCACATGCTCCTA	GATAAGGCTTGGCAACCCAAGTAA
Tnfα	TATGGCCCAGACCCTCACA	GGAGTAGACAAGGTACAACCCATC
Mcp1	AGCAGCAGGTGTCCCAAAGA	GTGCTGAAGACCTTAGGGCAGA
Cd11b	CCACTCATTGTGGGCAGCTC	GGGCAGCTTCATTCATCATGTC
Cd11c	AGGTCTGCTGCTGCTGGCTA	GGTCCCGTCTGAGACAAACTG
F4/80	TTGCAAAGTCCTGTGTGCTC	TGCCATCAACTCATGATACCCT
Ly6c	TGCCTGCAACCTTGTCTGAG	GCTGGGCAGGAAGTCTCAAT
Ly6g	TTGCAAAGTCCTGTGTGCTC	GTCCAGAGTGGGGCAGA
Fbgα	TGTGGAGAGACATCAGAGTCAATG	CGTCAATCAACCCTTTCATCC
Tf	TGTGCACCGAGCAATGGAA	GCTTGCACAGAGATATGCA
Pai1	TGCTGAACTCATCAGACAATGGAAG	TCGGCCAGGGTTGCACTAA
Bip	GAACCAACTCACGTCCAA	GCAATAGTGCCAGCATCT
Atf4	GCCTGACTCTGCTGCTTA	GCCTTACGGACCTCTTC
Xbp1	CTGAGTCCGAATCAGGTGCAG	GTCCATGGGAAGATGTTCTGG
Atf6	TTCCCAGGATTTCAGCAGGTT	TCAGCATCAGGAATGCGTGT
Chop	TCCCTGCCTTTCACCTTG	CGTTCTCCTGCTCCTTCTC
Hif1a	TCAAGTCAGCAACGTGGAAG	TATCGAGGCTGTGTCGACTG
Ho1	CCTCACTGGCAGGAAATCATC	CCTCGTGGAGACGCTTTACATA
Mnsod	GCACATTAACGCGCAGATCA	AGCCTCCAGCAACTCTCCTT

Table 2 Primer sequences for real-time PCR.

	Fibrinogen (mg/dl)	D-dimer (μg/ml)
ND	<50	<0.1
	79	<0.1
	148	<0.1
	143	<0.1
HFD1	<50	
	<50	
	<50	
	<50	
HFD2	<50	
	<50	
	116	
	98	
HFD4	80	<0.1
	163	<0.1
	135	<0.1
	120	<0.1

100 μg / body of LPS (Lipopolysaccharide from E. coli 0111: B4, Chondrex, Inc., WA, U.S.A.) was administered as a PC, and blood sample was collected 24 hours later. Fibrinogen: 261 mg / dl, D-dimer: 0.32 μg / ml

Table 3　Plasma fibrinogen and D-dimer.

Figure Legend for Supplementary Figure

Suppl. Figure.1 8-OHdG immunostaining in ND and HFD-fed mice.

(A) Liver histological images of ND and HFD-fed mice. 4x objective's scale bar: 200μm. 10x objective's scale bar: 50μm. 20x objective's scale bar: 20μm.

(B) Liver histological images of ND and HFD-fed mice 24 h after Con A administration. 4x objective's scale bar: 200μm. 10x objective's scale bar: 50μm. 20x objective's scale bar: 20μm.

Suppl. Figure.2 Hepatic mRNA expression.

Intrahepatic mRNA expression levels were measured by qRT-PCR. Expression levels of the respective mRNAs are normalized to that of GAPDH and normalized data are presented as fold change compared with Control of ND-fed mice. The data are shown as means ± SD. * $P<0.05$ vs. Control of ND-fed mice.

Supplementary Figure. 1

(A)

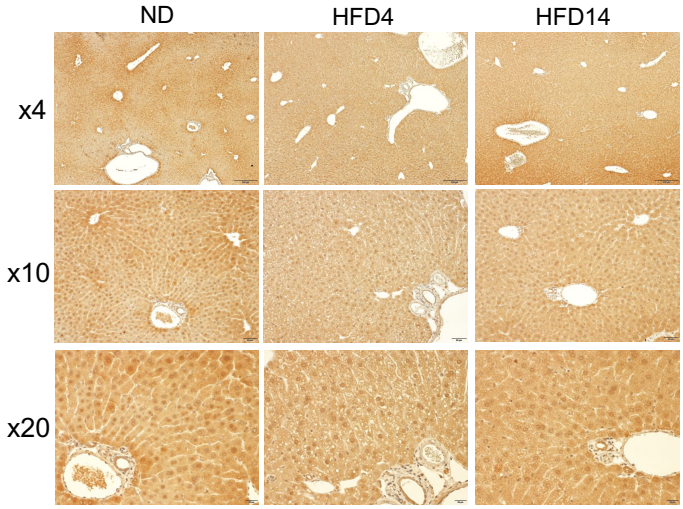

(B)

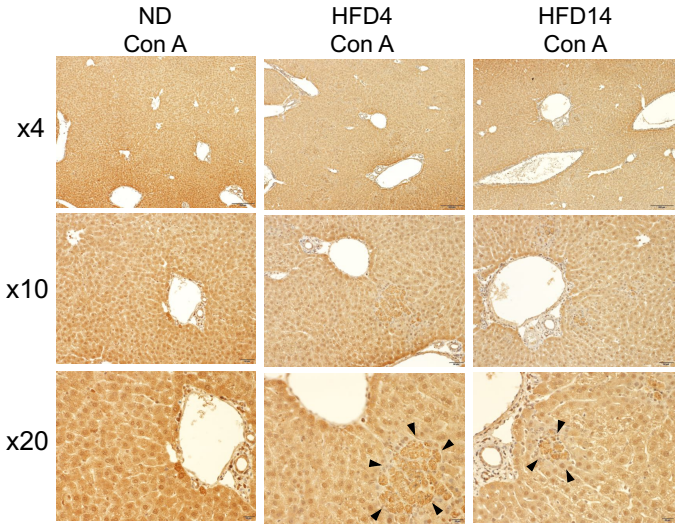

Supplementary Figure. 2

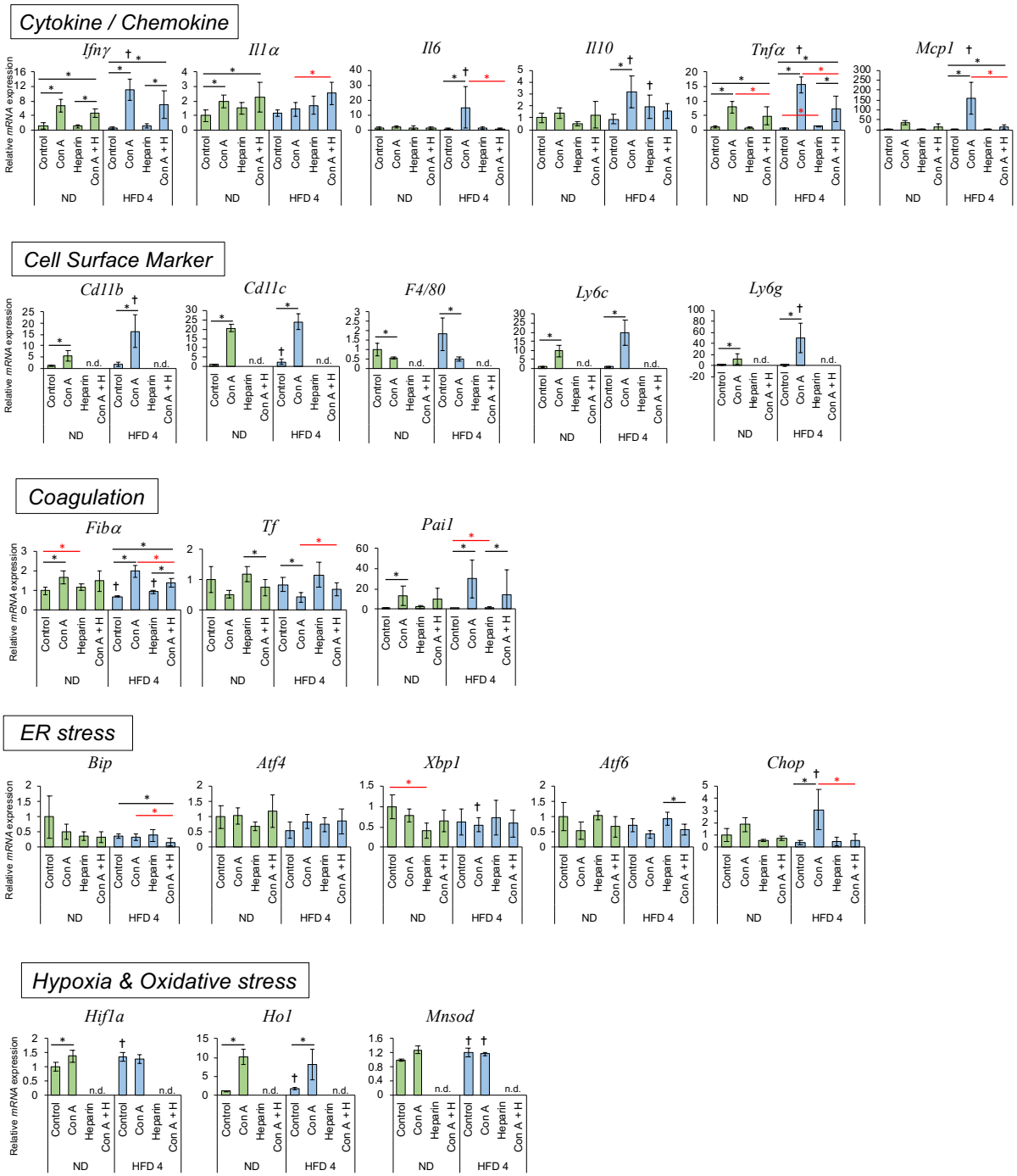

	ND 8 weeks	HFD4 8 weeks	HFD14 8 weeks
Body weight (g)	22.25 ± 1.39	25.11 ± 1.11 *	26.21 ± 1.4 *
Fig.1			
Serum			
ALT (U/l)	28.40 ± 5.27	27.83 ± 8.47	30.17 ± 9.77
T-Cho (mg/dl)	66.40 ± 14.62	161.33 ± 7.03 *	170.83 ± 15.25 *
TG (mg/dl)	35.60 ± 10.31	53.50 ± 18.65	91.17 ± 45.83 *
Glu (mg/dl)	179.00 ± 68.50	314.33 ± 87.7 *	319.83 ± 72.37 *
Fig. 3			
Serum			
ALT (U/l)			
Control	32.00 ± 1.73	33.00 ± 9.54	32.00 ± 7.94
Con A	302.00 ± 227.48	4674.50 ± 2210.72 *	3349.50 ± 2209.21 *
Fig. 4			
Serum			
ALT (U/l)			
Control	25.17 ± 7.68	26.83 ± 9.83	
Con A 1h	37.20 ± 10.03	61.00 ± 32.02	
Con A 3h	75.60 ± 35.91	101.17 ± 47.81	
Con A 24h	158.80 ± 169.39	3319.20 ± 961.60 *	
Fig. 5			
Serum			
ALT (U/l)			
Con A	434.17 ± 174.97	5934.33 ± 2705.53 *	
Con A + Heparin	36.33 ± 9.27	111.86 ± 78.22	

Supplementary Table 1 Body weight and actual measured value of each experiment.